Antonello Merlino[1]
Luigi Vitagliano[2]
Marc Antoine Ceruso[3]
Alfredo Di Nola[4]
Lelio Mazzarella[1,2]
[1] *Dipartimento di Chimica, Università degli Studi di Napoli "Federico II," Via Cinthia, 80125 Napoli, Italy*

[2] *Centro di Studio di Biocristallografia, CNR, Via Mezzocannone 6, 80134 Napoli, Italy*

[3] *Department of Physiology and Biophysics, Mt Sinai School of Medicine, One Gustave L. Levy Place, New York, NY 11104, USA*

[4] *Dipartimento di Chimica, Università "La Sapienza," P. le A. Moro 5, 00185 Roma, Italy*

Global and Local Motions in Ribonuclease A: A Molecular Dynamics Study

Received 30 January 2002; accepted 22 May 2002

Abstract: *The understanding of protein dynamics is one of the major goals of structural biology. A direct link between protein dynamics and function has been provided by x-ray studies performed on ribonuclease A (RNase A) (B. F. Rasmussen et al.,* Nature*, 1992, Vol. 357, pp. 423–424; L. Vitagliano et al.,* Proteins: Structure, Function, and Genetics*, 2002, Vol. 46, pp. 97–104). Here we report a 3 ns molecular dynamics simulation of RNase A in water aimed at characterizing the dynamical behavior of the enzyme. The analysis of local and global motions provides interesting insight on the dynamics/function relationship of RNase A. In agreement with previous crystallographic reports, the present study confirms that the RNase A active site is constituted by rigid (His12, Asn44, Thr45) and flexible (Lys41, Asp83, His119, Asp121) residues. The analysis of the global motions, performed using essential dynamics, shows that the two β-sheet regions of RNase A move coherently in opposite directions, thus modifying solvent accessibility of the active site, and that the mixed α/3_{10}-helix (residues 50–60) behaves as a mechanical hinge during the breathing motion of the protein. These data demonstrate that this motion, essential for RNase A substrate binding and release, is an intrinsic dynamical property of the ligand-free enzyme.* © 2002 Wiley Periodicals, Inc. Biopolymers 65: 274–283, 2002

Keywords: *ribonucleases; protein dynamics; protein structure–function; molecular dynamics; essential dynamics*

Correspondence to: Lelio Mazzarella; email: mazzarella@chemistry.unina.it

Contract grant sponsor: MURST PRIN and CNR Agenzia2000

INTRODUCTION

Bovine pancreatic ribonuclease (RNase A) has been used as a model in several fundamental studies in biochemistry and biophysics,[1,2] It was the first enzyme for which a complete amino acid sequence was determined,[3] and the third enzyme whose three-dimensional structure was solved by x-ray crystallography.[4] Despite the enormous amount of data collected on RNase A, several recent findings have stimulated a renewed interest in this enzyme. In particular, the discovery that several enzymes that belong to the pancreatic-like ribonuclease superfamily are endowed with special biological functions[5,6] has stimulated the design of RNase A derivatives with antitumoral and cytotoxic activities.[6,7] Furthermore, structural studies carried out on RNase A and its dimeric counterpart bovine seminal ribonuclease have provided important insights into the mechanisms that regulate the three-dimensional (3D) domain swapping.[8–12] In this framework, the very recent x-ray structure determination of a 3D domain swapping dimer of RNase A has also suggested an intriguing mechanism for amyloid fiber formation.[12]

Studies on RNase A have provided important information on the role played by the dynamical properties of the enzymes on their catalytic efficiency. In a seminal paper, Petsko and co-workers used RNase A to show the most direct experimental evidence between dynamics and function.[13,14] Along this line, we have recently demonstrated, by using x-ray crystallography, that RNase A undergoes subtle but significant domain motions upon binding and release of a substrate analog.[15] Similar domain motions have been observed in RNase A structures derived from crystals kept in low humidity environments.[16,17]

The dynamical properties of RNase A have been investigated by molecular dynamics (MD) simulations.[18–21] MD produces atomic trajectories that allow the understanding and interpretation of experimental results and the capability to interpolate or extrapolate experimental data into regions hardly accessible experimentally.

RNase A MD simulations were carried out for a rather short period of time ($\leq$150 ps). Given the importance of the simulation time scale,[22] we have carried out a 3 ns MD simulation of RNase A in water. Here we describe the local motions of important regions as well as global motions as derived by essential dynamics (ED) analyses. In particular, the mobility of the active site region is in line with their functional role derived from crystallographic[23] and site-directed mutagenesis[2] studies. Furthermore, the analysis of the global dynamical properties shows that the breathing motion of the two β-sheets regions of RNase A, which is crucial for substrate binding and release,[15] is an intrinsic dynamical feature of the ligand-free enzyme.

METHODS

System

The structure of RNase A consists of two antiparallel β-sheets, which form a characteristic V-shaped motif and of three helices that are packed against the β-sheets[24] (Figure 1). The two arms, which constitute the V-shaped motif, will be hereafter denoted as V_1 and V_2. In particular, V_1 is made up of residues 61–63, 71–75, and 105–111, 116–124; and V_2 are made up of residues 42–46, 82–87, and 96–101. The three helices encompass residues 3–13 (helix I), 25–35 (helix II), and 50–60 (helix III).

Molecular Dynamics

The MD simulation has been performed by using the GROMACS software package.[25] The x-ray structure of RNase A (Protein Data Bank entry code 7rsa) determined at 1.26 Å resolution by Wlodawer et al.[26] has been used as starting model. As far as the double conformation side chains are concerned, the rotamer with the highest occupancy was considered. The protein and the water molecules reported in the x-ray structure were immersed in a rectangular box of $52 \times 62 \times 49$ Å^3, filled with 4155 additional water molecules. The total volume of the protein/solvent box used in the simulation is approximately 178 nm^3, whereas the protein volume is approximately 7.6 nm^3. It can be estimated that more than 20 layers of water separate the protein from the box edge. The ionization state of charged residues was set to mimic a neutral pH environment. All Lys

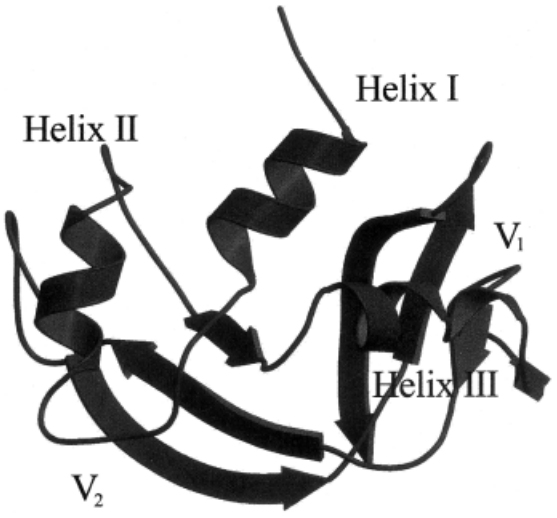

FIGURE 1 Ribbon diagram of RNase A structure. The V_1 and V_2 arms (see text for the definition) and the helices are labeled.

and Arg residues were positively charged, whereas Asp and Glu residues were negatively charged. The protonation state of the histidine residues was derived from recently refined structure of RNase A at six different pHs performed at atomic resolution.[27] From these data, it was shown that, at neutral pH, His12, His119, and His48 were uncharged. In particular, His12 and His48 were protonated at $N^{\delta 1}$, whereas His119 was protonated at $N^{\epsilon 2}$. Furthermore, the fully exposed His105, for which the protonation state could not be assessed, was assumed to be protonated at $N^{\epsilon 2}$ only. With these assumptions the net charge of the protein was +4. In order to make the overall system neutral, four water molecules were replaced by chloride ions. The simulation was carried out on a system containing 14,264 atoms, of which 1231 were protein atoms, 13,029 water atoms, and 4 chloride ions. The energy of the system was minimized by fixing the protein and the crystallographic water oxygens. The resulting model was submitted to 20 ps of molecular dynamics with a starting temperature of 300 K. The energy was then minimized without restrained, before starting constant temperature molecular dynamics at 300 K. A 3 ns simulation was performed. Bond lengths were constrained by the SHAKE procedure[28] and nonbonded interactions were evaluated using a cutoff of 10 Å for Lennard–Jones and a 13 Å one for Coulomb potentials. A dielectric constant of $\epsilon = 1$ was used to model the electrostatic interaction of the system. A single point charge (SPC) water model was used for the solvent molecules in the simulation. The integration time step was set to 0.002 ps and the coordinates were saved every 0.2 ps. The trajectory was checked to assess the quality of the simulation using GROMACS routines and in-house programs. To identify hydrogen bonds, both donor–acceptor (D-A) distances (<3.5 Å) and D—H · · · A angles (>110°) were checked. All the interactions reported as hydrogen bonds in the text satisfy both criteria.

Essential Dynamics

To characterize global motions of protein segments, essential degrees of freedom were extracted according to the essential dynamics method.[29,30] The essential dynamics (ED) method, often referred to as principal component analysis (PCA), is based on the multivariate analysis. ED does not imply any hypothesis on the shape of the energy surface as required in the normal modes analysis. ED is based on the construction of the covariance matrix of the coordinate fluctuations. After diagonalization of the matrix, a set of eigenvectors and eigenvalues is obtained as output. The eigenvectors represent the directions of motions and the eigenvalues the amount of motion along each eigenvector. The eigenvectors are then sorted according to their eigenvalues in descending order. Frequently, the first ten eigenvectors account for about the 80% of the overall fluctuation.

The covariance matrix of the positional fluctuations was constructed using only C^{α} atoms. To determine the structural response of RNase A where small perturbation are introduced, mechanical response matrix was built from the above covariance matrix.[31,32]

In order to demonstrate that a good convergence in the essential space had been reached in our simulation, root mean square inner product (RMSIP) between two halves of the equilibrated trajectory was calculated as described by Di Nola and co-workers[33,34].

The RMSIP is defined as

$$[1/10 \sum_{i=1,\,10} \sum_{j=1,\,10} (\eta_i^{a}\, \eta_j^{b})^2]^{1/2}$$

where η_i^{a} and η_j^{b} are the *i*th and *j*th eigenvectors from the first and second half of the equilibrated trajectory, respectively.

RESULTS AND DISCUSSION

Structural Stability and Comparison with the Experimentally Determined Structures

The overall structural stability of the protein during the simulation has been monitored using several properties. The root mean square deviations (RMSD) of the model coordinates during the simulation vs the starting x-ray structure as function of time are reported in Figure 2 for both main- and side-chain atoms.

Figure 2 shows that the overall deviation of each MD structure from the crystal one reaches a *plateau* in about one nanosecond. The deviation is ~0.2 and ~0.3 nm, for the backbone and the side chains, respectively.

Accordingly, the remaining 2000 ps were used for subsequent analyses. Similar trends are observed for other parameters, such as radius of gyration, total accessible surface, and total number of hydrogen bonds, which were used as global structural controls (data not shown). It is worth noting that the average

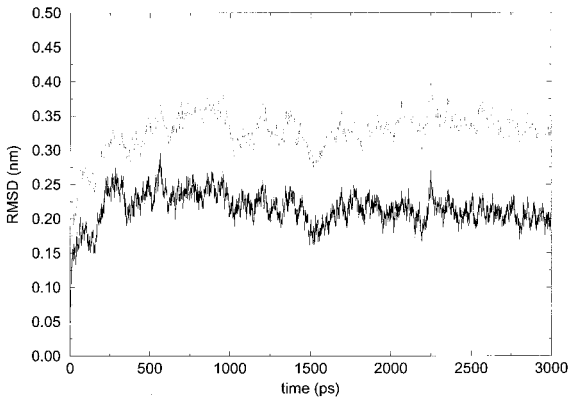

FIGURE 2 Main-chain (black line) and side-chain (gray line) RMSD from the starting x-ray structure as function of time.

Table I MD Average of Some Geometrical Properties of RNase A Compared with the Corresponding X-Ray and NMR Values[a]

	X-Ray	NMR	MD
Gyration radius of C^{α} structure (Å)	11.74	11.66 (0.07)	11.64 (0.11)
Accessible surface Area (nm^2)	30.27	30.85 (0.68)	30.60 (0.91)

[a] Standard deviations in parentheses.

values of the radius of gyration and the total accessible surface are very similar to the experimentally determined values (Table I). To compare the global structure of RNase A derived from the MD simulation with those determined by x-ray crystallography (XRNaseA)[26] and NMR (NMRRNaseA),[35] an average conformation (MDRNaseA) was derived from the plateau region (from 1.0 to 3.0 ns) of the simulation. MDRNaseA and the experimentally determined structures are very similar. In fact, the RMSD, computed on C^{α} atoms, of MDRNaseA vs XRNaseA and NMRRNaseA are 1.79 and 1.82 Å, respectively. The larger differences are located in the loop regions (residues 1–3, 21–23, 37–39, 65–70, 92–94, 112–115), whereas very small deviations occur in the secondary structure regions (data not shown). Similar trends are observed when the NMR structure is compared to the crystalline one.[35]

Fluctuations During Simulation

To describe the motions about the mean conformation, C^{α} root mean square fluctuations (RMSF) were evaluated for each residue of the polypeptide chain (Figure 3a). As for the RMSD, regular secondary structure regions show low mobility during the simulation, whereas pronounced fluctuations are observed for loop residues (1–4, 22–24, 37–39, 56–57, 66–71, 88–94, 112–114). The RMSF were compared to the atomic mobility of the x-ray model as derived from the B factors (Figure 3b). The analysis of Figures 3a and 3b reveals that the two plots present a similar trend across the sequence, despite the differences in the environmental condition of the protein molecule in the x-ray and MD studies (pH, hydration level, and crystal packing effects). In these two panels some fragments are rather different. However, these are confined to the residues 75–85 and 100–110.

Active Site Motions

Previous crystallographic studies carried out on ligand-free and complexed RNase A[23] have shown that the active site of the enzyme consists of flexible and rigid residues. In particular, residues such as Lys41, His119, and Gln11 display high mobility whereas His12 and Thr45 are more rigid. The mobility of these residues in the present simulation has been monitored by the analysis of the evolution of the side-chain hydrogen-bond contacts.

In Figure 4a the time evolution of the hydrogen-bond distance between the $N^{\delta 1}$ atom of His12 and the backbone oxygen of Thr45 is reported. In agreement with literature data,[23,36,37] the plot shows that this hydrogen bond is very stable during simulation. This finding suggests that this bond significantly contributes to the high rigidity of this active site region.

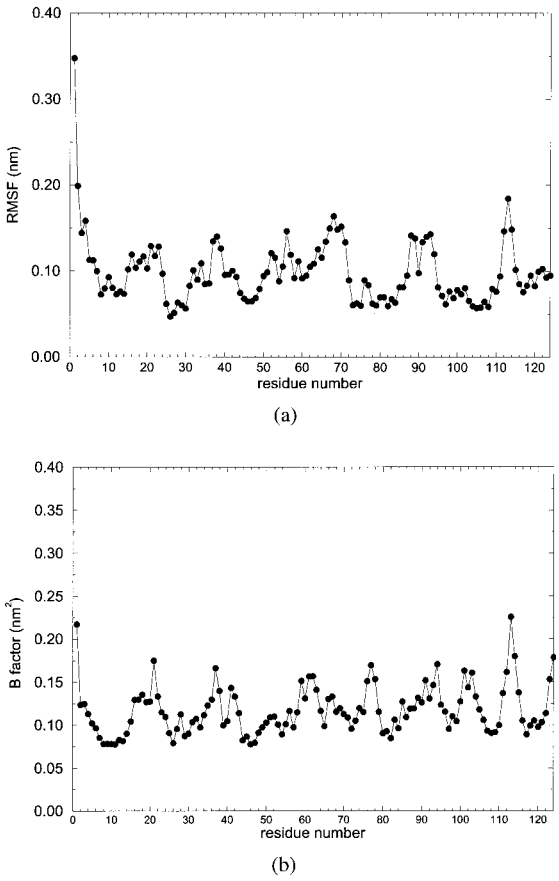

FIGURE 3 (a) Root mean square fluctuations of C^{α} atoms in the equilibrated region of the trajectory. (b) B factors of C^{α} atoms in the starting x-ray structure.

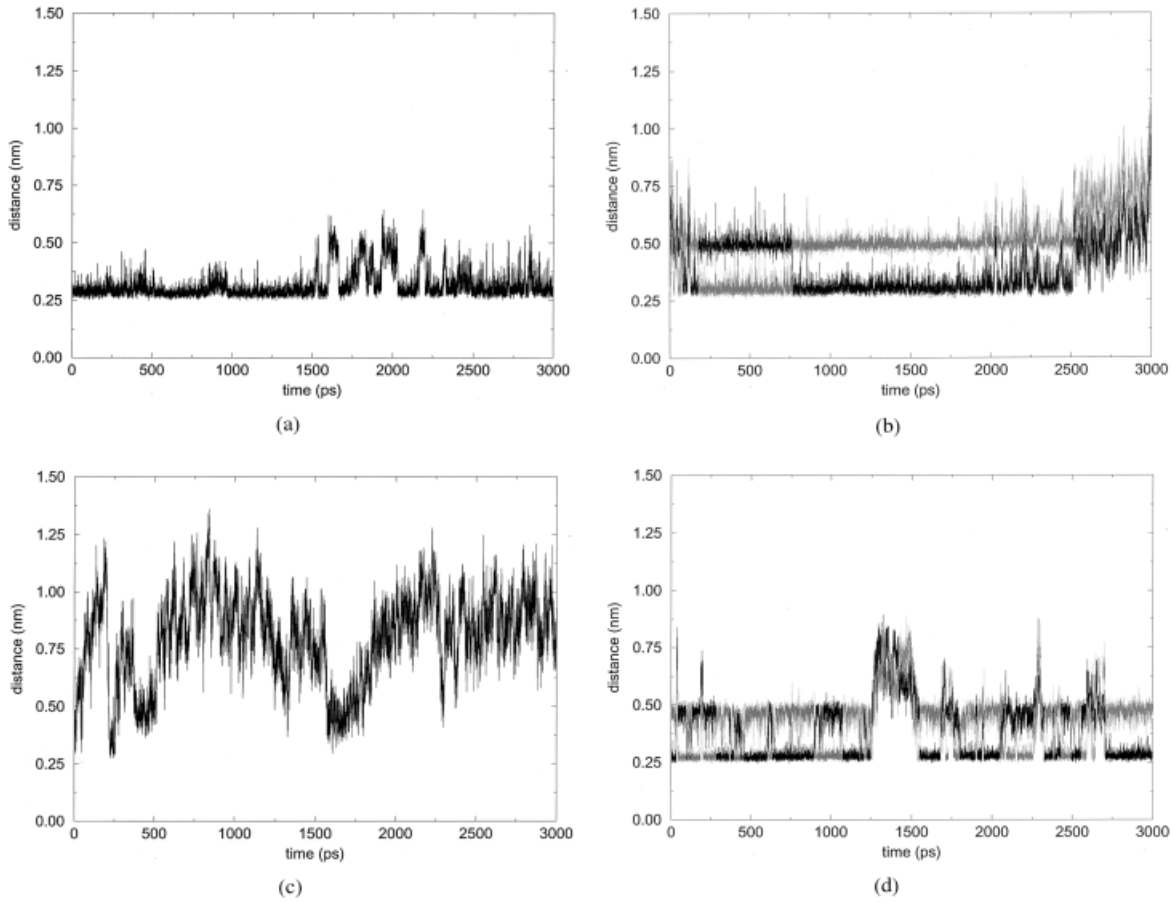

FIGURE 4 Distances between selected atoms of the active site as function of time: (a) $N^{\delta 1}$ His12–Thr45; (b) $N^{\epsilon 2}$ His 119-$O^{\delta 1}$Asp 121 (black), $N^{\epsilon 2}$ His119–$O^{\delta 2}$ Asp121 (gray); (c) N^{ζ}Lys 41–$O^{\delta 1}$ Asn44; (d) $O^{\gamma 1}$Thr45–$O^{\delta 1}$ Asp83 (black), $O^{\gamma 1}$Thr45–$O^{\delta 2}$ Asp83 (gray).

On the other hand, the monitoring of the hydrogen bond between His119 and Asp121 side chains reveals that this bond is occasionally broken during the simulation and lost in the last 500 ps (Figure 4b). This is in agreement with crystallographic studies on ligand-free RNase A that have indicated that this interaction is not particularly strong as His119 adopts two different conformations.[23] Notably, we have recently shown that the strength of the bond increases when a ligand is located in the P1 site.[38] It is worth noting that this hydrogen bond was not observed in a previous simulation of free enzyme,[18] but it was observed in MD simulation of RNase A complexes.[18] The present simulation shows that, indeed, a transitory hydrogen bond between His119 and Asp121 side chains is formed in the ligand-free RNase A. The transient character of this bond supports the hypothesis of Raines and co-workers[39–41] that the hydrogen bond formed between His119 and Asp121 cannot be considered as a low-barrier hydrogen bond like the one occurring in serine proteases.

The Lys41 side chain shows a high mobility during the simulation. We have recently proposed[38] that the Asn44 side chain, a highly conserved residue among ribonucleases,[42] may play a role in stabilizing the charged Lys41 side chain in proximity of the RNase A active site. The monitoring of the interactions between Asn44 and Lys41 side chains shows that a hydrogen bond was sporadically formed during the simulation (Figure 4c).

Although not directly involved in substrate binding, Asp83 is another residue that plays a significant role in the catalytic activity of RNase A.[43] During the MD simulation, the side chain of Asp83 forms a transient hydrogen bond with that of Thr45 (Figure 4d). Interestingly, structural studies[23,44,45] have shown that only when a uridine base is bound to the active site the carboxylate group of Asp83 forms this hydrogen bond. Indeed, such a bond cannot be formed when cytidine is bound to B1 subsite, since the $O^{\gamma 1}$ group of Thr45 donates a proton to the cytidine base.[46] The present data suggest that active site states

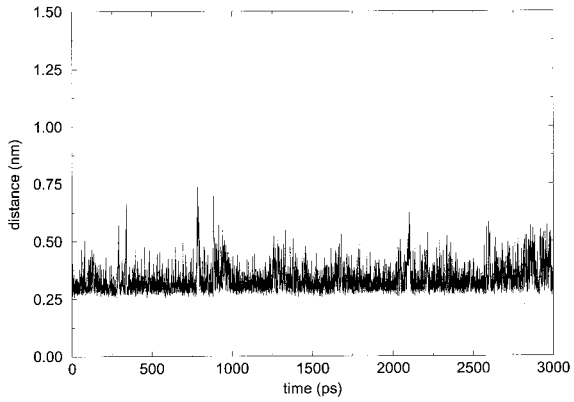

FIGURE 5 Distances between $O^{\delta 1}$ atom of Asn67 and N atom of Gln69 as function of time.

suitable for the binding of both bases are intrinsically accessible to the ligand-free RNase A.

Flexibility of the 65–72 Region

The loop region closed by the disulfide bridge Cys65–Cys72 is a region of RNase A that deserves particular attention. Several studies have proposed that this loop is one of the chain-folding initiation sites in the folding of RNase A.[47–50] Nevertheless, the analysis of the RMSF profile (Figure 3a) reveals that this is one of the most mobile regions of the protein. The intrinsic flexibility of this region has been further studied by monitoring the evolution of the hydrogen bonds that are important to confer stability to this loop region. Despite the large displacements of the loop throughout the simulation, the hydrogen bonds between O atom of Cys 65 and N atom of Gly 68, N atom of Cys 65 and the backbone O atom of Gln 69 (data not shown), and $O^{\delta 1}$ of Asn 67 and the backbone N atom of Gln 69 (Figure 5) are very stable showing that the local structure of the loop is rather rigid. This finding supports the recent hypothesis[50] that the correct folding of RNase A is influenced more by the local structure of the loop 65–72 than by the formation of the disulfide bridge 65–72.

Breathing Motion of RNase A

To characterize the global motions of protein fragments, we have analyzed the MD trajectory by essential dynamics.[30] Preliminarly, we checked the simulation convergence by using the RMSIP value as follows. The 2 ns equilibrated trajectory (see above) was divided in two halves of 1 ns each, and an ED analysis was performed for both of them. The RMSIP, computed considering ten eigenvectors for each half, was as high as 0.75. This indicates that the essential subspace obtained from one half of the equilibrated trajectory is similar to that calculated from the other, thus ensuring that a good convergence was reached in the simulation.

ED analysis performed on the whole equilibrated trajectory reveals that only 10 eigenvectors are sufficient to describe 80% of the fluctuations. As already reported for several other proteins,[30,32,33,51,52] the fluctuations of RNase A involve a limited set of directions in the essential subspace. To visualize the regions involved in these motions, the conformational evolution of RNase A along the first, the second, and the fifth principal components has been represented in a film-like fashion (Figures 6a–c). The atomic displacements observed for the first eigenvector are mainly concentrated in the regions of the loops 65–72 and 91–95 (Figure 6a). The motion of these two loops can be described as a circular movement on two different circles in opposite directions that points away from the protein core. In addition, as shown in Figure 6a, along the first eigenvector a concerted motion of V_1 and V_2 β-sheets (see Methods) is observed. The two β-sheets fluctuate coherently in opposite directions, thus modifying the solvent accessibility of the active site. The breathing motion of this region observed along the first eigenvector is very similar to that observed comparing ligand-free and complexed crystalline structures of RNase A.[15] This finding shows that the hinge bending motion, essential for RNase A substrate binding and release,[15] is an intrinsic dynamical property of the ligand-free enzyme. It is worth noting that this kind of movement has been already reported by a previous 150 ps MD simulation[21] and by crystallographic studies carried out on crystals kept in a low humidity environment.[16,17]

In order to measure the magnitude of this breathing motion upon ligand binding in the crystal, we had previously used the distance between N Thr45 and N Phe120.[15] These two residues, which are involved in the binding of the substrate, are placed on V_1 and V_2 arms of the β-sheet. In the present simulation, the distance between N Thr45 and N Phe120 fluctuates around a mean value of 9.03 Å with a standard deviation of 0.90 Å. This result is in close agreement with the observed variability of this distance in the x-ray structures of RNase A deposited in the Protein Data Bank. An exhaustive analysis on these structures reveals that this distance assumes values in the range 8.0–9.6Å. This breathing motion is also evident from the analysis of the third and fourth eigenvalues (data not shown).

Helix III as a Mechanical Hinge in the Breathing Motion of RNase A

The analysis of the motions corresponding to the second and the fifth eigenvector, represented in Fig-

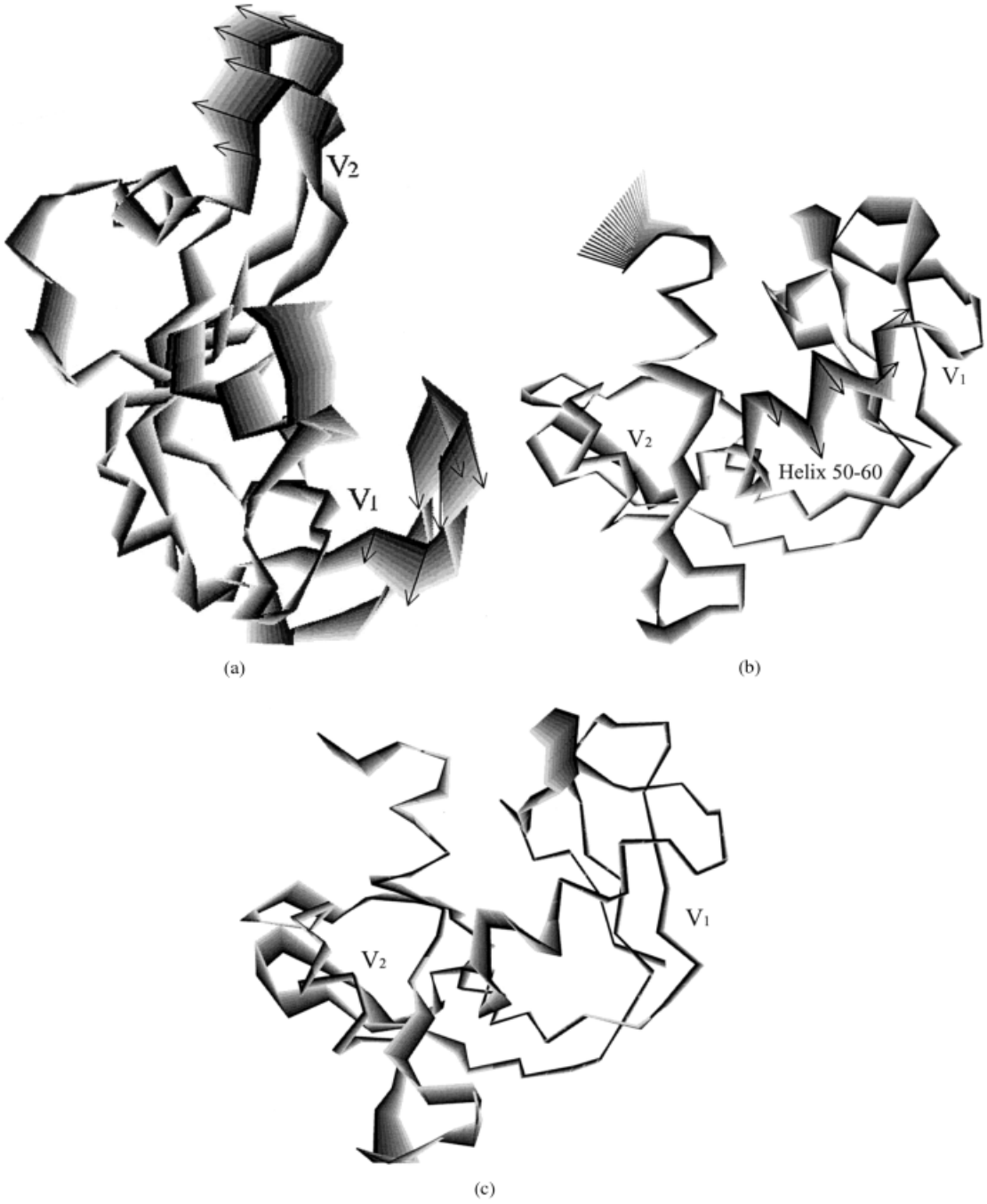

FIGURE 6 Protein motions along the first (a), the second (b), and the fifth (c) principal eigenvectors. A gray scale is used to represent motions in a film-like fashion. Vectors are used as qualitative indicators of the direction of C^{α} atom motions.

ures 6b and 6c, reveals novel features of the dynamical behavior of RNase A. In both cases, the main displacements are localized in loops 16–22 and 91–95 and in helix 50–60. The motion of the helix III is particularly interesting since this helix joins the two β-sheets. During the simulation helix III clearly splits into two distinct segments, formed by residues 50–55 and residues 56–60, which fluctuate independently (Figures 6b and 6c). Moreover, helix III of MDRNaseA structure is very similar to that found in NMRRNaseA structures and quite different to that found in XRNaseA. On the basis of the structural fluctuations of helix 50–60, we suggest that the center of this element can act as a bending point that regulates the

breathing motion of the two β-sheets. It is worth noting that α-helices have been found to behave as mechanical hinges in other proteins such as in aspartate aminotrasferase and in glyceraldeide-3-phosphate dehydrogenase.[53]

Interestingly, in all structures so far reported for RNase A, helix III is actually a mixed helix, with residues 50–56 in α-helical conformation and residues 57–60 forming a 3_{10} -helix. It is worth mentioning that the mixed character of this helix is preserved during the simulation (Figures 7a and 7b). The switching point from one helical motif to the other coincides with the bending point identified in the present study. Therefore, these results point out that mixed helices can act as mechanical hinges. This observation is particularly suggestive, as mixed helices are a rather common structural motif in globular proteins.[54,55]

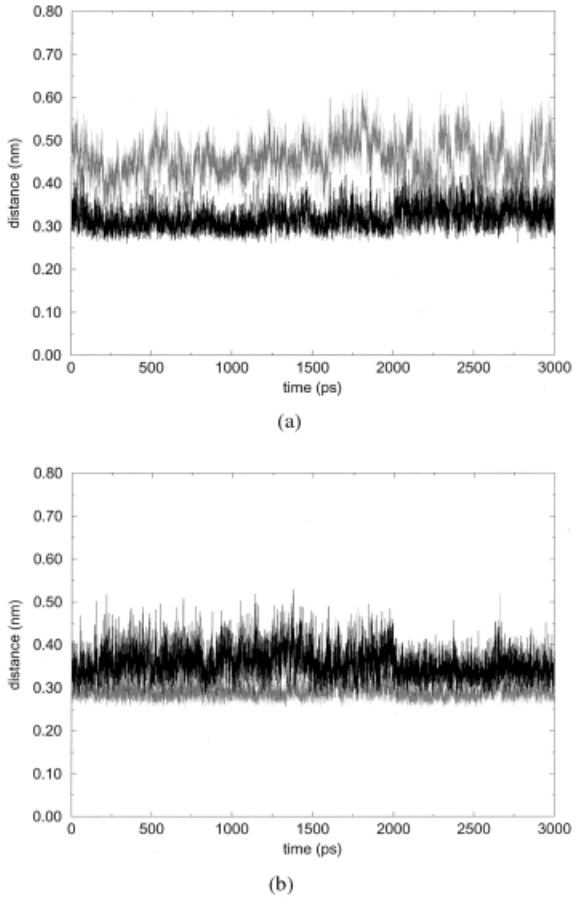

FIGURE 7 Distances between selected atoms of helix III as function of time. (a) The distances between O55–N58 (i, $i+3$ interaction) and O55–N59 (i, $i+4$ interaction) are reported in black and gray, respectively. (b) The distances between O51–N54 (i, $i+3$ interaction) and O51–N55 (i, $i+4$ interaction) are reported in black and gray, respectively.

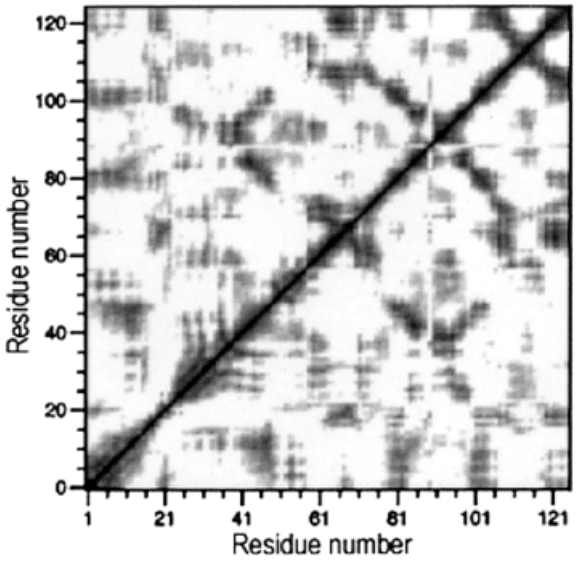

FIGURE 8 Mechanical response matrix. Residue numbers are reported on the horizontal and vertical axes. Intense correlations correspond to dark regions.

Correlated Motions Derived from the Mechanical Response Matrix

To investigate the structural response of RNase A structure to small perturbations, a mechanical response matrix (Figure 8), calculated from the fluctuation of the C^{α} atoms, was constructed as reported by Chillemi et al.[32] In the matrix, black regions correspond to protein segments with coherent motions. Figure 8 shows that correlation of structural element motions reflect the topological organization of the protein.[33]

The matrix shows that the fluctuations of the N-terminal helix I are strictly related to those of the V_2 region. This result is not surprising since the N-terminal helix is bound to the V_2 by two strong hydrogen bonds formed by Gln11 and His12 with Asn44 and Thr45, respectively. It is interesting to note that according to Scheraga and co-workers[56] the intramolecular interactions between helix I and the V_2 region play an important role in favoring the correct folding of RNase A. Furthermore, the diagram also shows that the N-terminal residues of helix III (residues 50–56) essentially follows the motions of the V_2 arm. On the other hand, the motions of helix II are not associated to the movements of other rigid fragments of RNase A. Finally, the movement of loop 65–72 is correlated to the V_1 arm. Indeed, loop 65–72 is anchored to the V_1 by the strong hydrogen bond[57,58] between Lys66 N and Asp121 $O^{\delta 2}$, which is well conserved during the simulation.

CONCLUSIONS

In the present paper we report the results of a 3 ns MD simulation of RNase A in water. The analysis of the local motions of active site residues provides further support to the hypotheses on their catalytic role put forward on the bases of recent site-directed mutagenesis and crystallographic experiments.[2,30,41] The ED analysis of the trajectory provides a detailed picture of the intrinsic mobility of rigid segments of the protein. The present data confirm the β-sheet breathing motion observed by crystallographic experiments.[15–17,44] Although these motions were already reported in a short time scale MD simulation,[21] the present simulation, based on a more adequate sampling of the conformational space of the protein, increases the reliability of these results. Moreover, in the present study these β-sheet motions have been also linked to the mobility of other rigid elements of RNase A. In particular, the ED analysis have shown that helix III, which is a mixed $\alpha/3_{10}$-helix, behaves as a mechanical hinge during the breathing motion of the protein. This behavior may be ascribed to the fact that helix III is directly linked to both the V_1 (through the disulfide bridge 58–110) and the V_2 (through the fragment 46–50) arms of RNase A. It is likely that these structural constraints are responsible for the mixed $\alpha/3_{10}$-character of the helix. In this context, it is worth mentioning that the dynamical properties here identified may be a common feature of pancreatic-like ribonucleases, since this $\alpha/3_{10}$-helix and the disulfide bridge linking V_1 to helix III are conserved motifs in all known structures of ribonucleases.

The structural similarities between the breathing motion reported here and those associated to the binding and the release of a substrate analog[15] suggest that intrinsic dynamical properties of RNase A are used by the enzyme to perform its catalytic action. Therefore, according to the scheme of Nussinov and co-workers,[59] the ligand binding to RNase A produces a population shift of the conformational states accessible to the enzyme.

It is likely that this intrinsic flexibility may be strongly reduced at a very low temperature. Therefore, the inability of RNase A to bind substrate analogs at temperatures below 220 K[13] may be ascribed to the loss of the protein flexibility highlighted by the present MD simulation. Finally, the detailed characterization of the dynamical properties of RNase A is an essential prerequisite for the understanding of the dynamical properties of RNase A dimers,[10,12] which have provided important insights into the mechanisms of the 3D domain swapping and of the amyloid fiber formation.[60]

The authors are indebted to Mr. L. De Luca for his precious help with some of the computations. This work was financially supported by the MURST PRIN and by CNR Agenzia2000.

REFERENCES

1. Blackburn, P.; Moore, S. In The Enzymes; Boyer, P. D., Ed; Academic Press: New York,1982; pp 317–433.
2. Raines, R.T. Chem Rev 1998, 98, 1045–1065.
3. Smyth, D.G.; Stein, W.H.; Moore, S. J Biol Chem 1963, 238, 277–234.
4. Kartha, G.; Bello, J.; Harker, D. Nature 1967, 213, 862–865.
5. D'Alessio, G.; Di Donato, A.; Mazzarella, L.; Piccoli, R. In Ribonucleases: Structures and Functions; Riordan, J. F., D'Alessio, G., Eds.; Academic Press: New York,1997; pp 383–423.
6. Youle, R. J.; D'Alessio, G. In Ribonuclease:Structures and functions; D'Alessio, G., Riordan, J. F., Eds.; Academic Press: New York, 1996; pp 491–514.
7. Leland, P. A.; Schultz, L. W.; Kim, B. M.; Raines, R. T. Proc Natl Acad Sci USA 1998, 95, 10407–10412.
8. Mazzarella, L.; Capasso, S.; Demasi, D.; Di Lorenzo, G.; Mattia, C. A.; Zagari, A. Acta Cryst D 1993, 49, 389–402.
9. Mazzarella, L.; Vitagliano, L.; Zagari, A. Proc Natl Acad Sci USA 1995, 92, 3799–3803.
10. Liu, Y.; Hart, P. J.; Schlunegger, M. P.; Eisenberg, D. Proc Natl Acad Sci USA 1998, 95, 3437–3442.
11. Vitagliano, L.; Adinolfi, S.; Sica, F.; Merlino, A.; Zagari, A.; Mazzarella, L. J Mol Biol 1999, 293, 569–577.
12. Liu, Y.; Gotte, G.; Libonati, M.; Eisenberg, D. Nat Struct Biol 2001, 8, 211–214.
13. Rasmussen, B. F.; Stock, A. M.; Ringe, D.; Petsko, G. A. Nature 1992, 357, 423–424.
14. Tilton, R. F. J.; Dewan, J. C.; Petsko, G. A. Biochemistry 1992, 31, 2469–2481.
15. Vitagliano, L.; Merlino, A.; Zagari, A.; Mazzarella, L. Proteins Struct Funct Genet 2002, 46,97–104.
16. Radha Kishan, K. V.; Chandra, N. R.; Sudarsanakumar, C.; Suguna, K.; Vijayan, M. Acta Cryst D 1995, 51, 703–710.
17. Sadasivan, C.; Nagendra, H. G.; Vijayan, M. Acta Cryst D 1998, 54,1343–1352.
18. Brunger, A. T.; Brooks, C. L.; Karplus, M. Proc Natl Acad Sci USA 1985, 82, 8458–8462.
19. Seshadri, K.; Rao, V. S.; Vishveshwara, S. J Biomol Struct Dynam 1994, 12, 581–603.
20. Nadig, G.; Ratnaparkhi, G. S.; Varadarajan, R.; Vishveshwara, S. Protein Sci 1996, 5, 2104–2114.
21. Nadig, G.; Vishveshwara, S. Biopolymers 1997, 42, 505–520.
22. Doniach, S.; Eastman, P. Curr Opin Struct Biol 1999, 9, 157–163.
23. Gilliland, G. In Ribonuclease:Structures and Functions; D'Alessio, G., Riordan, J. F., Eds.; Academic Press: New York, 1997; pp 306–341

24. Wlodawer, A.; Bott, R.; Sjolin, L. J Biol Chem 1982, 257, 1325–1332.
25. van der Spoel, D.; van Druner, R.; Berendsen, H. J. C. GROningen MAchine for Chemical Simulation, Department of Biophysical Chemistry, BIOSON Research Institute, Groningen, 1994.
26. Wlodawer, A.; Svenson, L. A.; Sjolin, L.; Gilliland, G. L. Biochemistry 1988, 27, 2705–2717
27. Berisio, R.; Lamzin, V. S.; Sica, F.; Wilson, K. S.; Zagari, A.; Mazzarella, L. J Mol Biol 1999, 292, 845–854.
28. Ryckaert, J. P.; Ciccotti, G.; Berendsen, H. J. C. J Comput Phys 1977, 23, 327–341.
29. Garcia, A. E. Phys Rev Lett 1992, 68, 2696–2699.
30. Amadei, A.; Linssen, A. B.; Berendsen, H. J. Proteins 1993, 17, 412–425.
31. Wong, C. F.; Zheng, C.; Shen, J, McCammon, A.; Wolynes, P. G. J Phys Chem 1993, 97, 3100–3110.
32. Chillemi, G.; Falconi, M.; Amadei, A.; Zimatore, G.; Desideri, A.; Di Nola, A. Biophys J 1997, 73, 1007–1018.
33. Ceruso, M. A.; Amadei, A.; Di Nola, A. Protein Sci 1999, 8, 147–160.
34. Amadei, A.; Ceruso, M. A.; Di Nola, A. Proteins Struct Funct Genet 1999, 36, 419–424.
35. Santoro, J.; Gonzalez, C.; Bruix, M.; Neira, J. L.; Nieto, J. L.; Herranz, J.; Rico, M. J Mol Biol 1993, 229, 722–734.
36. Wlodawer, A. In Biological Macromolecules and Assembly; Jurnak, F., McPherson, A., Eds.; Wiley: New York, 1985; pp 394–439.
37. Fedorov, A. A.; Joseph-McCarthy, D.; Fedorov, E.; Sirakova, D.; Graf, I.; Almo, S. C. Biochemistry 1996, 35, 15962–15979.
38. Vitagliano, L.; Merlino, A.; Zagari, A.; Mazzarella, L. Protein Sci 2000, 9, 1217–1225.
39. Quirk, D. J.; Park, C.; Thompson, J. E.; Raines, R. T. Biochemistry 1998, 37, 17958–17964.
40. Quirk, D. J.; Raines, R. T. Biophys J 1999, 76, 1571–1579.
41. Schultz, L. W.; Quirk, D. J.; Raines, R. T. Biochemistry 1998, 37, 8886–8898.
42. Beintema, J. J.; Schueller, C.; Irie, M.; Carsana, A. Prog Biophys Mol Biol 1988, 51, 165–192.
43. delCardayre, S. B.; Raines, R. T. J Mol Biol 1995, 252, 328–336.
44. Vitagliano, L.; Adinolfi, S.; Riccio, A.; Sica, F.; Zagari, A.; Mazzarella, L. Protein Sci 1998, 7, 1691–1699.
45. Wladkowski, B. D.; Svensson, L. A.; Sjolin, L.; Ladner, J. E.; Gilliland, G. L. J Am Chem Soc 1993, 120, 5488–5498.
46. Zegers, I.; Maes, D.; Dao-Thi, M. H.; Poortmans, F.; Palmer, R.; Wyns, L. Protein Sci 1994, 3, 2322–1339.
47. Nemethy, G.; Scheraga, H. A. Proc Natl Acad USA 1979, 76, 6050–6054.
48. Capasso, S.; Di Donato, A.; Esposito, L.; Sica, F.; Sorrentino,G.; Vitagliano, L.; Zagari, A.; Mazzarella, L. J Mol Biol 1996, 257, 492–496.
49. Xu, X.; Rothwarf, D. M.; Scheraga, H. A. Biochemistry 1996, 35, 6406–6417.
50. Orrù, S.; Vitagliano, L.; Esposito, L.; Mazzarella, L.; Marino, G.; Ruoppolo, M. Protein Sci 2000, 9,2577–2582.
51. van Aalten, D. M.; Findlay, J. B.; Amadei, A.; Berendsen, H. J. Protein Eng 1995, 8, 1129–1135.
52. van Aalten, D. M.; Amadei, A.; Linssen, A. B.; Eijsink, V. G.; Vriend, G.; Berendsen, H. J. Proteins 1995, 22, 45–54.
53. Hayward, S. Proteins Struct Funct Genet 1999, 36, 425–435.
54. Barlow, D. J.; Thornton, J. M. J Mol Biol 1988,201,601–619.
55. Benedetti, E.; Di Blasio, B.; Pavone, V.; Pedone, C.; Toniolo, C.; Crisma, M. Biopolymers 1992, 32, 453–456.
56. Laity, J. H.; Montelione, G. T.; Scheraga, H. A. Biochemistry 1999, 38, 16432–16442.
57. Baker, W. R.; Kintanar, A. Arch Biochem Biophys 1996, 327, 189–199.
58. Esposito, L.; Vitagliano, L. Sica, F.; Sorrentino, G.; Zagari, A.; Mazzarella, L. J Mol Biol 2000, 297, 713–732.
59. Kumar, S. M.; Buyong, M.; Tsai, C. J.; Sinha, N.; Nussinov, R. Protein Sci 2000, 9,10–19.
60. Newcomer, M. E. Nature Struct Biol 2001, 8, 282–284.